arXiv:nucl-ex/0307023 v1 28 Jul 2003

ρ^0 Production and Possible Modification in Au+Au and p+p Collisions at $\sqrt{s_{NN}} = 200$ GeV

J. Adams,[3] C. Adler,[12] M.M. Aggarwal,[25] Z. Ahammed,[28] J. Amonett,[17] B.D. Anderson,[17] M. Anderson,[5] D. Arkhipkin,[11] G.S. Averichev,[10] S.K. Badyal,[16] J. Balewski,[13] O. Barannikova,[28,10] L.S. Barnby,[17] J. Baudot,[15] S. Bekele,[24] V.V. Belaga,[10] R. Bellwied,[41] J. Berger,[12] B.I. Bezverkhny,[43] S. Bhardwaj,[29] P. Bhaskar,[38] A.K. Bhati,[25] H. Bichsel,[40] A. Billmeier,[41] L.C. Bland,[2] C.O. Blyth,[3] B.E. Bonner,[30] M. Botje,[23] A. Boucham,[34] A. Brandin,[21] A. Bravar,[2] R.V. Cadman,[1] X.Z. Cai,[33] H. Caines,[43] M. Calderón de la Barca Sánchez,[2] A. Cardenas,[28] J. Carroll,[18] J. Castillo,[18] M. Castro,[41] D. Cebra,[5] P. Chaloupka,[9] S. Chattopadhyay,[38] H.F. Chen,[32] Y. Chen,[6] S.P. Chernenko,[10] M. Cherney,[8] A. Chikanian,[43] B. Choi,[36] W. Christie,[2] J.P. Coffin,[15] T.M. Cormier,[41] J.G. Cramer,[40] H.J. Crawford,[4] D. Das,[38] S. Das,[38] A.A. Derevschikov,[27] L. Didenko,[2] T. Dietel,[12] X. Dong,[32,18] J.E. Draper,[5] F. Du,[43] A.K. Dubey,[14] V.B. Dunin,[10] J.C. Dunlop,[2] M.R. Dutta Majumdar,[38] V. Eckardt,[19] L.G. Efimov,[10] V. Emelianov,[21] J. Engelage,[4] G. Eppley,[30] B. Erazmus,[34] P. Fachini,[2] V. Faine,[2] J. Faivre,[15] R. Fatemi,[13] K. Filimonov,[18] P. Filip,[9] E. Finch,[43] Y. Fisyak,[2] D. Flierl,[12] K.J. Foley,[2] J. Fu,[42] C.A. Gagliardi,[35] M.S. Ganti,[38] T.D. Gutierrez,[5] N. Gagunashvili,[10] J. Gans,[43] L. Gaudichet,[34] M. Germain,[15] F. Geurts,[30] V. Ghazikhanian,[6] P. Ghosh,[38] J.E. Gonzalez,[6] O. Grachov,[41] V. Grigoriev,[21] S. Gronstal,[8] D. Grosnick,[37] M. Guedon,[15] S.M. Guertin,[6] A. Gupta,[16] E. Gushin,[21] T.J. Hallman,[2] D. Hardtke,[18] J.W. Harris,[43] M. Heinz,[43] T.W. Henry,[35] S. Heppelmann,[26] T. Herston,[28] B. Hippolyte,[43] A. Hirsch,[28] E. Hjort,[18] G.W. Hoffmann,[36] M. Horsley,[43] H.Z. Huang,[6] S.L. Huang,[32] T.J. Humanic,[24] G. Igo,[6] A. Ishihara,[36] P. Jacobs,[18] W.W. Jacobs,[13] M. Janik,[39] I. Johnson,[18] P.G. Jones,[3] E.G. Judd,[4] S. Kabana,[43] M. Kaneta,[18] M. Kaplan,[7] D. Keane,[17] J. Kiryluk,[6] A. Kisiel,[39] J. Klay,[18] S.R. Klein,[18] A. Klyachko,[13] D.D. Koetke,[37] T. Kollegger,[12] A.S. Konstantinov,[27] M. Kopytine,[17] L. Kotchenda,[21] A.D. Kovalenko,[10] M. Kramer,[22] P. Kravtsov,[21] K. Krueger,[1] C. Kuhn,[15] A.I. Kulikov,[10] A. Kumar,[25] G.J. Kunde,[43] C.L. Kunz,[7] R.Kh. Kutuev,[11] A.A. Kuznetsov,[10] M.A.C. Lamont,[3] J.M. Landgraf,[2] S. Lange,[12] C.P. Lansdell,[36] B. Lasiuk,[43] F. Laue,[2] J. Lauret,[2] A. Lebedev,[2] R. Lednický,[10] V.M. Leontiev,[27] M.J. LeVine,[2] C. Li,[32] Q. Li,[41] S.J. Lindenbaum,[22] M.A. Lisa,[24] F. Liu,[42] L. Liu,[42] Z. Liu,[42] Q.J. Liu,[40] T. Ljubicic,[2] W.J. Llope,[30] H. Long,[6] R.S. Longacre,[2] M. Lopez-Noriega,[24] W.A. Love,[2] T. Ludlam,[2] D. Lynn,[2] J. Ma,[6] Y.G. Ma,[33] D. Magestro,[24] S. Mahajan,[16] L.K. Mangotra,[16] D.P. Mahapatra,[14] R. Majka,[43] R. Manweiler,[37] S. Margetis,[17] C. Markert,[43] L. Martin,[34] J. Marx,[18] H.S. Matis,[18] Yu.A. Matulenko,[27] T.S. McShane,[8] F. Meissner,[18] Yu. Melnick,[27] A. Meschanin,[27] M. Messer,[2] M.L. Miller,[43] Z. Milosevich,[7] N.G. Minaev,[27] C. Mironov,[17] D. Mishra,[14] J. Mitchell,[30] B. Mohanty,[38] L. Molnar,[28] C.F. Moore,[36] M.J. Mora-Corral,[19] V. Morozov,[18] M.M. de Moura,[41] M.G. Munhoz,[31] B.K. Nandi,[38] S.K. Nayak,[16] T.K. Nayak,[38] J.M. Nelson,[3] P. Nevski,[2] V.A. Nikitin,[11] L.V. Nogach,[27] B. Norman,[17] S.B. Nurushev,[27] G. Odyniec,[18] A. Ogawa,[2] V. Okorokov,[21] M. Oldenburg,[18] D. Olson,[18] G. Paic,[24] S.U. Pandey,[41] S.K. Pal,[38] Y. Panebratsev,[10] S.Y. Panitkin,[2] A.I. Pavlinov,[41] T. Pawlak,[39] V. Perevoztchikov,[2] W. Peryt,[39] V.A. Petrov,[11] S.C. Phatak,[14] R. Picha,[5] M. Planinic,[44] J. Pluta,[39] N. Porile,[28] J. Porter,[2] A.M. Poskanzer,[18] M. Potekhin,[2] E. Potrebenikova,[10] B.V.K.S. Potukuchi,[16] D. Prindle,[40] C. Pruneau,[41] J. Putschke,[19] G. Rai,[18] G. Rakness,[13] R. Raniwala,[29] S. Raniwala,[29] O. Ravel,[34] R.L. Ray,[36] S.V. Razin,[10,13] D. Reichhold,[28] J.G. Reid,[40] G. Renault,[34] F. Retiere,[18] A. Ridiger,[21] H.G. Ritter,[18] J.B. Roberts,[30] O.V. Rogachevski,[10] J.L. Romero,[5] A. Rose,[41] C. Roy,[34] L.J. Ruan,[32,2] V. Rykov,[41] R. Sahoo,[14] I. Sakrejda,[18] S. Salur,[43] J. Sandweiss,[43] I. Savin,[11] J. Schambach,[36] R.P. Scharenberg,[28] N. Schmitz,[19] L.S. Schroeder,[18] K. Schweda,[18] J. Seger,[8] D. Seliverstov,[21] P. Seyboth,[19] E. Shahaliev,[10] M. Shao,[32] M. Sharma,[25] K.E. Shestermanov,[27] S.S. Shimanskii,[10] R.N. Singaraju,[38] F. Simon,[19] G. Skoro,[10] N. Smirnov,[43] R. Snellings,[23] G. Sood,[25] P. Sorensen,[6] J. Sowinski,[13] H.M. Spinka,[1] B. Srivastava,[28] S. Stanislaus,[37] R. Stock,[12] A. Stolpovsky,[41] M. Strikhanov,[21] B. Stringfellow,[28] C. Struck,[12] A.A.P. Suaide,[41] E. Sugarbaker,[24] C. Suire,[2] M. Šumbera,[9] B. Surrow,[2] T.J.M. Symons,[18] A. Szanto de Toledo,[31] P. Szarwas,[39] A. Tai,[6] J. Takahashi,[31] A.H. Tang,[2,23] D. Thein,[6] J.H. Thomas,[18] V. Tikhomirov,[21] M. Tokarev,[10] M.B. Tonjes,[20] T.A. Trainor,[40] S. Trentalange,[6] R.E. Tribble,[35] M.D. Trivedi,[38] V. Trofimov,[21] O. Tsai,[6] T. Ullrich,[2] D.G. Underwood,[1] G. Van Buren,[2] A.M. VanderMolen,[20] A.N. Vasiliev,[27] M. Vasiliev,[35] S.E. Vigdor,[13] Y.P. Viyogi,[38] S.A. Voloshin,[41] W. Waggoner,[8] F. Wang,[28] G. Wang,[17] X.L. Wang,[32] Z.M. Wang,[32] H. Ward,[36] J.W. Watson,[17] R. Wells,[24] G.D. Westfall,[20] C. Whitten Jr.,[6] H. Wieman,[18] R. Willson,[24] S.W. Wissink,[13] R. Witt,[43] J. Wood,[6] J. Wu,[32] N. Xu,[18] Z. Xu,[2] Z.Z. Xu,[32] A.E. Yakutin,[27] E. Yamamoto,[18] J. Yang,[6] P. Yepes,[30] V.I. Yurevich,[10] Y.V. Zanevski,[10] I. Zborovský,[9] H. Zhang,[43,2] H.Y. Zhang,[17] W.M. Zhang,[17] Z.P. Zhang,[32] P.A. Żołnierczuk,[13] R. Zoulkarneev,[11] J. Zoulkarneeva,[11] and A.N. Zubarev[10]

(STAR Collaboration)[*]

[1]Argonne National Laboratory, Argonne, Illinois 60439
[2]Brookhaven National Laboratory, Upton, New York 11973
[3]University of Birmingham, Birmingham, United Kingdom
[4]University of California, Berkeley, California 94720
[5]University of California, Davis, California 95616
[6]University of California, Los Angeles, California 90095
[7]Carnegie Mellon University, Pittsburgh, Pennsylvania 15213
[8]Creighton University, Omaha, Nebraska 68178
[9]Nuclear Physics Institute AS CR, Řež/Prague, Czech Republic
[10]Laboratory for High Energy (JINR), Dubna, Russia
[11]Particle Physics Laboratory (JINR), Dubna, Russia
[12]University of Frankfurt, Frankfurt, Germany
[13]Indiana University, Bloomington, Indiana 47408
[14]Insitute of Physics, Bhubaneswar 751005, India
[15]Institut de Recherches Subatomiques, Strasbourg, France
[16]University of Jammu, Jammu 180001, India
[17]Kent State University, Kent, Ohio 44242
[18]Lawrence Berkeley National Laboratory, Berkeley, California 94720
[19]Max-Planck-Institut für Physik, Munich, Germany
[20]Michigan State University, East Lansing, Michigan 48824
[21]Moscow Engineering Physics Institute, Moscow Russia
[22]City College of New York, New York City, New York 10031
[23]NIKHEF, Amsterdam, The Netherlands
[24]Ohio State University, Columbus, Ohio 43210
[25]Panjab University, Chandigarh 160014, India
[26]Pennsylvania State University, University Park, Pennsylvania 16802
[27]Institute of High Energy Physics, Protvino, Russia
[28]Purdue University, West Lafayette, Indiana 47907
[29]University of Rajasthan, Jaipur 302004, India
[30]Rice University, Houston, Texas 77251
[31]Universidade de São Paulo, São Paulo, Brazil
[32]University of Science & Technology of China, Anhui 230027, China
[33]Shanghai Institute of Nuclear Research, Shanghai 201800, P.R. China
[34]SUBATECH, Nantes, France
[35]Texas A & M, College Station, Texas 77843
[36]University of Texas, Austin, Texas 78712
[37]Valparaiso University, Valparaiso, Indiana 46383
[38]Variable Energy Cyclotron Centre, Kolkata 700064, India
[39]Warsaw University of Technology, Warsaw, Poland
[40]University of Washington, Seattle, Washington 98195
[41]Wayne State University, Detroit, Michigan 48201
[42]Institute of Particle Physics, CCNU (HZNU), Wuhan, 430079 China
[43]Yale University, New Haven, Connecticut 06520
[44]University of Zagreb, Zagreb, HR-10002, Croatia

(Dated: July 28, 2003)

We report results on $\rho(770)^0 \to \pi^+\pi^-$ production at mid-rapidity in p+p and peripheral Au+Au collisions at $\sqrt{s_{NN}} = 200$ GeV. This is the first direct measurement of $\rho(770)^0 \to \pi^+\pi^-$ in heavy-ion collisions. The ρ^0 mass is significantly shifted in minimum bias p+p and peripheral Au+Au interactions. The ρ^0 mass shift is dependent on transverse momentum and multiplicity. The modification of the ρ^0 meson mass, width, and shape due to phase space and dynamical effects are discussed.

PACS numbers: 25.75.Dw,25.75.-q,13.85.Hd

In-medium modification of the ρ meson due to the effects of increasing temperature and density has been proposed as a possible signal of a phase transition of nuclear matter to a deconfined plasma of quarks and gluons, which is expected to be accompanied by the restoration of chiral symmetry [1].

The ρ^0 meson measured in the dilepton channel probes all stages of the system formed in relativistic heavy-ion collisions because the dileptons have negligible final state interactions with the hadronic environment. Heavy-ion experiments at CERN indicate an enhanced dilepton production cross section in the invariant mass range of 200-

*URL: www.star.bnl.gov

600 MeV/c^2 [2]. Even though various models with different approaches have successfully reproduced this observation [1], the experimental results are so far inconclusive with regard to the magnitude of the possible in-medium modification of the ρ^0 mass. The study of the dilepton decay channel currently relies on model calculations based on a so-called "hadronic cocktail", a superposition of the expected contributions to the dilepton spectrum [3]. The present hadronic decay measurement, $\rho(770)^0 \to \pi^+\pi^-$, is the first of its kind in heavy-ion collisions, and provides experimental data to help constrain the input to the hadronic cocktail used for such studies.

Even in the absence of the phase transition, at normal nuclear density, temperature and density dependent modifications of the ρ^0 meson are expected to be measurable. Effects such as phase space [4, 5, 6, 7, 8, 9, 10] and dynamical interactions with matter [6, 8, 10] may modify the ρ^0 mass, width, and shape. These modifications of the ρ^0 properties take place close to kinetic freeze-out (vanishing elastic collisions), in a dilute hadronic gas at late stages of heavy-ion collisions. At such low matter density, the proposed modifications are expected to be small, but observable. The effects of phase space due to the rescattering of pions, $\pi^+\pi^- \to \rho^0 \to \pi^+\pi^-$, and Bose-Einstein correlations between pions from ρ^0 decay and pions in the surrounding matter are present in p+p [5, 6, 8, 11] and Au+Au [4, 6, 7, 8, 9, 10] collisions. The interference between different pion scattering channels can effectively distort the line shape of resonances [12]. Dynamical effects due to the ρ^0 interacting with the surrounding matter are also expected to be present in p+p and Au+Au interactions, and have been evaluated for the latter [6, 8, 10].

Since the ρ^0 lifetime of $c\tau = 1.3$ fm is small with respect to the lifetime of the system formed in Au+Au collisions, the ρ^0 meson is expected to decay, regenerate, and rescatter all the way through kinetic freeze-out. In the context of statistical models, the measured ρ^0 yield should reflect conditions at kinetic freeze-out rather than at chemical freeze-out (vanishing inelastic collisions) [6, 8, 9, 13]. In p+p collisions, the ρ^0 meson is expected to be produced predominatly by string fragmentation. The measurement of the ρ^0 meson in p+p and Au+Au interactions at the same nucleon-nucleon cms energy can provide valuable insight for understanding the dynamics of these distinct, complex systems.

The detector system used for these studies was the Solenoidal Tracker at RHIC (STAR). The main tracking device within STAR is the time projection chamber (TPC) [14] located inside a 0.5 T solenoidal magnetic field. In addition to providing momentum information, the TPC provides particle identification for charged particles by measuring their ionization energy loss (dE/dx). In Au+Au collisions, a minimum bias trigger was defined using coincidences between two zero degree calorimeters that measured the spectator neutrons. In p+p collisions, the minimum bias trigger was defined using coincidences between two beam-beam counters that measured the charged particle multiplicity in forward pseudorapidities ($3.3 < |\eta| < 5.0$). This trigger is sensitive to non-singly diffractive (NSD) events, with negligible bias on yields [15]. Approximately 11 million minimum bias p+p events, 1.5 million high multiplicity p+p events, and 1.2 million events in the peripheral centrality class corresponding to 40-80% of the inelastic hadronic Au+Au cross section were used for this analysis. The beam energy was $\sqrt{s_{NN}} = 200$ GeV. High multiplicity p+p events were those from the top 10% of the minimum bias p+p multiplicity distribution for $|\eta| < 0.5$. Since the pion daughters from ρ^0 decays originate at the interaction point, only tracks whose distance of closest approach to the primary interaction vertex was less than 3 cm were selected. Charged pions were selected by requiring their dE/dx to be within three standard deviations (3σ) of the expected mean. In order to enhance track quality [16], candidate decay daughters were also required to have $|\eta| < 0.8$ and transverse momenta (p_T) greater than 0.2 GeV/c.

The main focus of this study was the decay channel $\rho^0 \to \pi^+\pi^-$, which has a branching ratio of $\sim$100%. Similar to previous e^+e^- and p+p measurements, the ρ^0 sample studied did not select exclusively on the ℓ=1 $\pi^+\pi^-$ channel [17, 18, 19, 20, 21, 22, 23, 24, 25]. The measurement was performed calculating the invariant mass for each $\pi^+\pi^-$ pair in an event. The resulting invariant mass distribution was then compared to a reference distribution calculated from the geometric mean of the invariant mass distributions obtained from uncorrelated $\pi^+\pi^+$ and $\pi^-\pi^-$ pairs from the same events. The $\pi^+\pi^-$ invariant mass distribution ($M_{\pi\pi}$) and the like-sign reference distribution were normalized to each other at $M_{\pi\pi} \gtrsim 1.5$ GeV/c^2. The resulting raw distributions, after like-sign subtraction, for minimum bias p+p and peripheral Au+Au collisions at mid-rapidity ($|y| \leq 0.5$) for a particular p_T bin are shown in Fig. 1. The p_T coverage of the $\pi^+\pi^-$ pair is $0.2 \leq p_T \leq 2.8$ GeV/c for minimum bias p+p and $0.2 \leq p_T \leq 2.2$ GeV/c for peripheral Au+Au collisions.

The solid black line in Fig. 1 is the sum of all the contributions in the hadronic cocktail. The K^0_S was fit to a Gaussian (dotted line). The ω (light grey line) and $K^*(892)^0$ (dash-dotted line) shapes were obtained from the HIJING event generator [26], with the kaon being misidentified as a pion in the case of the K^{*0}. The $\rho^0(770)$ (dashed line), the $f_0(980)$ (dotted line) and the $f_2(1270)$ (dark grey line) were fit by relativistic Breit-Wigner functions [27] BW $= M_{\pi\pi}M_0\Gamma/[(M_0^2 - M_{\pi\pi}^2)^2 + M_0^2\Gamma^2]$ times the Boltzmann factor [5, 6, 7, 8] PS $= (M_{\pi\pi}/\sqrt{M_{\pi\pi}^2 + p_T^2}) \times \exp(-\sqrt{M_{\pi\pi}^2 + p_T^2}/T)$ to account for phase space. Here, T is the temperature at which the resonance is emitted [6] and $\Gamma = \Gamma_0 \times (M_0/M_{\pi\pi}) \times [(M_{\pi\pi}^2 - 4m_\pi^2)/(M_0^2 - 4m_\pi^2)]^{(2\ell+1)/2}$ is the momentum dependent width [27]. The masses of K^0_S, ρ^0, f_0, and f_2 were free parameters in the fit, and the widths of ρ^0, f_0 and f_2 were fixed according to [28]. The uncorrected yields of K^0_S, ρ^0, ω, f_0, and f_2 were free parameters in the fit while the

K^{*0} fraction was fixed according to the $K^*(892)^0 \to \pi K$ measurement. The ρ^0, ω, K^{*0}, f_0, and f_2 distributions were corrected for the detector acceptance and efficiency determined from a detailed simulation of the TPC response using GEANT [16]. For the particular p_T bin depicted in Fig. 1 and the invariant mass region shown, this correction is approximately constant and is ∼25% for minimum bias p+p and varies from ∼25% to ∼35% for peripheral Au+Au collisions. The number of degrees of freedom (dof) from the fits was 196 and the typical χ^2/dof was 1.4. In the minimum bias p+p invariant mass distribution shown in Fig. 1, $\pi^\pm\pi^\pm$ Bose-Einstein correlations have been taken into account. These affect the distribution for $M_{\pi\pi} < 0.45$ GeV/c^2.

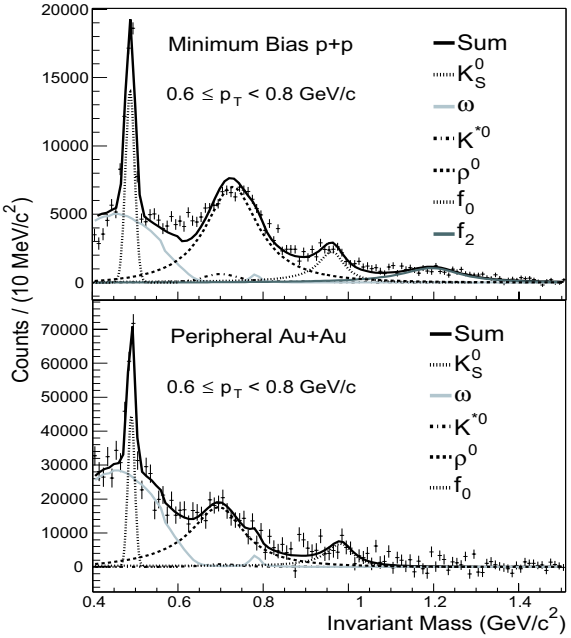

FIG. 1: The raw $\pi^+\pi^-$ invariant mass distributions after subtraction of the like-sign reference distribution for minimum bias p+p (top) and peripheral Au+Au (bottom) interactions.

The ρ^0 mass is shown as a function of p_T in Fig. 2 for peripheral Au+Au, high multiplicity p+p, and minimum bias p+p interactions. The ρ^0 mass was obtained by fitting the data to a relativistic p-wave ($\ell = 1$) Breit-Wigner function times a factor which accounts for phase space (BW×PS) in the hadronic cocktail. Since the phase space factor modifies the position of the peak for the BW function, the mass derived from the BW×PS fit may be shifted compared to the peak of the experimental invariant mass distribution and to the peak of the BW function alone. The ρ^0 peak was also fit to a relativistic p-wave BW function excluding the PS factor in the hadronic cocktail; however, the fit failed to reproduce the ρ^0 line shape, and underestimated the position of the peak in general, particularly at low p_T. This measurement does not have sufficient sensitivity to permit a systematic study of the ρ^0 width. Therefore, for the cocktail fits in this analysis, the ρ^0 width was fixed at $\Gamma_0 = 160$ MeV/c^2, consistent with folding the ρ^0 natural width (150.9 ± 2.0 MeV/c^2 [28]) with the intrinsic resolution of the detector [16]. In Au+Au collisions, the temperature used in the PS factor was $T = 120$ MeV [6], while in p+p, $T = 160$ MeV [29].

The ρ^0 mass at $|y| \leq 0.5$ for minimum bias p+p, high multiplicity p+p, and peripheral Au+Au collisions at $\sqrt{s} = 200$ GeV seems to increase as a function of p_T and is systematically lower than the value reported by [22]. The ρ^0 mass measured in peripheral Au+Au collisions is lower than the minimum bias p+p measurement. The ρ^0 mass for high multiplicity p+p interactions is lower than for minimum bias p+p interactions for all p_T bins, showing that the ρ^0 mass is also multiplicity dependent. Recent calculations are not able to reproduce the ρ^0 mass measured in peripheral Au+Au collisions without introducing in-medium modification of the ρ^0 meson [6, 7, 8, 9, 10].

Previous observations of the ρ meson in e^+e^- [30, 31, 32] and p+p interactions [22] indicate that the ρ^0 line shape is considerably distorted from a p-wave BW function. A mass shift of -30 MeV/c^2 or larger was observed in e^+e^- collisions at $\sqrt{s} = 90$ GeV [30, 31, 32]. In the p+p measurement at $\sqrt{s} = 27.5$ GeV [22], a ρ^0 mass of 0.7626 ± 0.0026 GeV/c^2 was obtained from a fit to the BW×PS function [11, 22]. However, in this measurement the position of the ρ^0 peak is lower than the average of the ρ^0 mass measured in e^+e^- interactions [28] by ∼30 MeV/c^2 [22]. This result is the only p+p measurement used in the hadro-produced ρ^0 mass average reported in [28].

In comparison to the in-medium ρ^0 production in hadronic Au+Au interactions, no modifications of the ρ^0 properties are expected for coherent ρ^0 production in ultra-peripheral heavy-ion collisions, where (in lowest order) at impact parameters $b > 2R_A$, a photon emitted by one gold ion fluctuates into a virtual ρ^0 meson state, which scatters diffractively from the other nucleus. The ρ^0 line shape in ultra-peripheral collisions measured with the STAR detector [27] is reproduced by a BW plus Söding interference term, with the ρ^0 mass and width consistent with their natural values reported in [28].

One uncertainty in the hadronic cocktail fit depicted in Fig. 1 is the possible existence of correlations of unknown origin near the ρ^0 mass. An example is correlations in the invariant mass distribution from particles like the $f_0(600)$ which are not well established [28]. The ω yield in the hadronic cocktail fits may account for some of these contributions and may cause the apparent decrease in the ρ^0/ω ratio between minimum bias p+p and peripheral Au+Au interactions. In order to evaluate the systematic uncertainty in the ρ^0 mass due to poorly known contributions in the hadronic cocktail, the ρ^0 mass was obtained by fitting the peak to the BW×PS function plus an exponential function representing these contributions. Using this procedure, the ρ^0 mass is systematically higher than the mass obtained from the hadronic cocktail fit. This

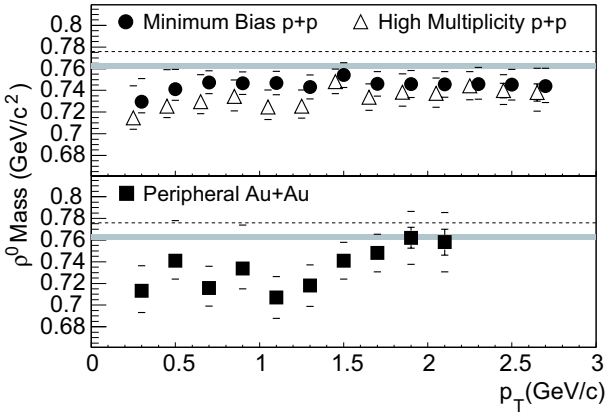

FIG. 2: The ρ^0 mass as a function of p_T for minimum bias p+p (filled circles), high multiplicity p+p (open triangles), and peripheral Au+Au (filled squares) collisions. The error bars indicate the systematic uncertainty. Statistical errors are negligible. The ρ^0 mass was obtained by fitting the data to the BW×PS functional form described in the text. The dashed lines represent the average of the ρ^0 mass measured in e^+e^- [28]. The shaded areas indicate the ρ^0 mass measured in p+p collisions [22]. The open triangles have been shifted downward on the abscissa by 50 MeV/c for clarity.

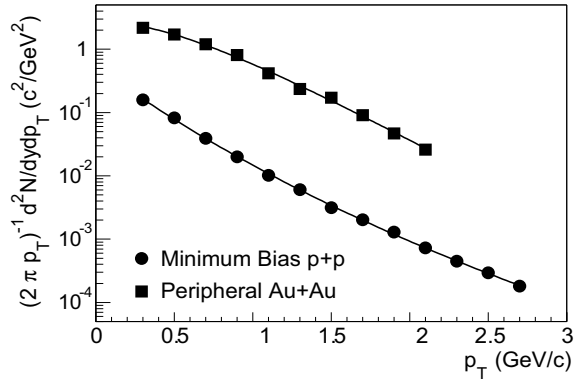

FIG. 3: The p_T distributions at mid-rapidity ($|y| < 0.5$) for ρ^0 mesons produced in minimum bias p+p and peripheral Au+Au interactions. See text for explanation on the functions used to fit the data. The errors shown are statistical only and are smaller than the symbols.

uncertainty is the main contribution to the systematic uncertainties shown in Fig. 2. Other contributions to the systematic errors shown in Fig. 2 result from uncertainty in the measurement of particle momenta (this leads to a mass resolution of $\sim$8 MeV/c^2 at the ρ^0 mass) and from the hadronic cocktail fits themselves. The systematic uncertainties are common to all p_T bins and are correlated between the p+p and peripheral Au+Au measurements.

The corrected invariant yields ($d^2N/(2\pi p_T dp_T dy)$) at $|y| < 0.5$ as a function of p_T for peripheral Au+Au and minimum bias p+p interactions are shown in Fig. 3. In p+p interactions, a power-law fit was used to extract the ρ^0 yield per unit of rapidity around mid-rapidity. The fit yielded $dN/dy = 0.252 \pm 0.002(\text{stat}) \pm 0.040(\text{syst})$ and $< p_T > = 0.634 \pm 0.003(\text{stat}) \pm 0.063(\text{syst})$ GeV/c. In Au+Au collisions, an exponential fit in $m_T - m_0$, where $m_0 = 0.769$ MeV/c^2 is the average ρ^0 mass reported in [28], was used to extract the ρ^0 yield and the inverse slope. The fit yielded $dN/dy = 5.9 \pm 0.1(\text{stat}) \pm 1.1(\text{syst})$ and an inverse slope of $319 \pm 4(\text{stat}) \pm 32(\text{syst})$ MeV ($< p_T > = 0.83 \pm 0.01(\text{stat}) \pm 0.08(\text{syst})$ GeV/c). The systematic errors quoted are due to uncertainties in the fits, the tracking efficiency, and the normalization between the $M_{\pi\pi}$ and the like-sign reference distributions.

The $d^2N/(2\pi p_T dp_T dy)$ distribution for p+p collisions is best fit to a power-law function. This behavior suggests that the ρ^0 production is dominated by hard processes at higher p_T.

The ρ^0/π^- ratio is $0.185 \pm 0.003(\text{stat}) \pm 0.035(\text{syst})$ for peripheral Au+Au, and $0.178 \pm 0.001(\text{stat}) \pm 0.028(\text{syst})$ for minimum bias p+p collisions. The comparison with measurements in e^+e^- [17, 18, 19], p+p [20, 21, 22, 23], K^+p [24], and π^-p [25] interactions at different cms energies is shown in Fig. 4. The ρ^0/π^- ratios from minimum bias p+p and peripheral Au+Au interactions are comparable.

The ρ^0/π^- ratios from statistical model calculations [8, 9, 13] for Au+Au collisions are considerably lower than the measurement presented in Fig. 4. The larger ρ^0/π^- ratio measured may be due to the interplay between the rescattering of the ρ^0 decay products and ρ^0 regeneration.

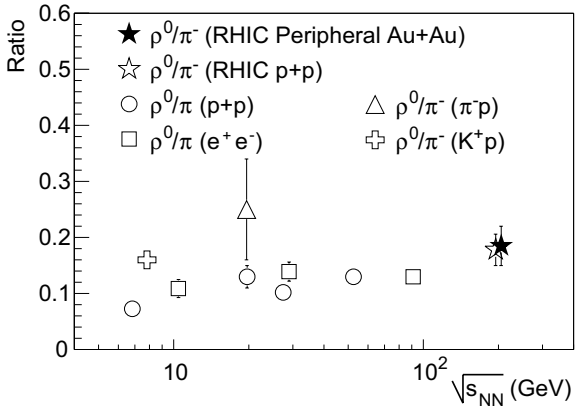

FIG. 4: ρ^0/π ratios as a function of cms energy. The ratios are from measurements in e^+e^- collisions at 10.45 GeV [17], 29 GeV [18] and 91 GeV [19] cms energy, p+p at 6.8 GeV [20], 19.7 GeV [21], 27.5 GeV [22] and 52.5 GeV [23], K^+p at 7.82 GeV [24] and π^-p at 19.6 GeV [25]. The errors on the ratios at $\sqrt{s_{NN}} = 200$ GeV are the quadratic sum of the statistical and systematic errors. The ratios at $\sqrt{s_{NN}} = 200$ GeV are offset from one another for clarity.

In conclusion, we have presented results on $\rho(770)^0$ production at mid-rapidity in minimum bias p+p and peripheral Au+Au collisions at $\sqrt{s_{NN}} = 200$ GeV. This is the first direct measurement of $\rho^0(770) \to \pi^+\pi^-$ in heavy-ion collisions. The ρ^0 mass seems to increase slightly as

a function of p_T, and to decrease with multiplicity. The measured ρ^0 peak in the invariant mass distribution is lower than previous measurements reported in [28] by $\sim$40 MeV/c^2 in minimum bias p+p interactions and $\sim$70 MeV/c^2 in peripheral Au+Au collisions. Similar mass shifts were observed in e^+e^- and p+p interactions. Dynamical interactions with the surrounding matter, interference between various $\pi^+\pi^-$ scattering channels, phase space distortions due to the rescattering of pions forming ρ^0, and Bose-Einstein correlations between ρ^0 decay daughters and pions in the surrounding matter are possible explanations for the apparent modification of the ρ^0 meson properties. The ρ^0/π^- ratio in peripheral Au+Au collisions is higher than predicted by statistical calculations, and is comparable to the measured value in minimum bias p+p interactions. Further measurements of the ρ^0 meson, along with other resonance particles, can be expected to provide important information on the dynamics of relativistic collisions and help in understanding the properties of nuclear matter under extreme conditions.

We thank the RHIC Operations Group and RCF at BNL, and the NERSC Center at LBNL for their support. This work was supported in part by the HENP Divisions of the Office of Science of the U.S. DOE; the U.S. NSF; the BMBF of Germany; IN2P3, RA, RPL, and EMN of France; EPSRC of the United Kingdom; FAPESP of Brazil; the Russian Ministry of Science and Technology; the Ministry of Education and the NNSFC of China; SFOM of the Czech Republic, DAE, DST, and CSIR of the Government of India; the Swiss NSF.

[1] R. Rapp and J. Wambach, Adv. Nucl. Phys. **25**, 1 (2000).
[2] G. Agakishiev *et al.*, Phys. Rev. Lett. **75**, 1272 (1995); B. Lenkeit *et al.*, Nucl. Phys. A **661**, 23 (1999).
[3] J. Kapusta, Nucl. Phys. A **715**, 709c (2003).
[4] H.W. Barz *et al.*, Phys. Lett. **B** 265, 219 (1991).
[5] P. Braun-Munzinger *et al.*, CERES Int. Note, March 2000, unpublished.
[6] E.V. Shuryak and G.E. Brown, Nucl. Phys. A **717**, 322 (2003).
[7] P.F. Kolb and M. Prakash, nucl-th/0301007.
[8] R. Rapp, hep-ph/0305011.
[9] W. Broniowski *et al.*, nucl-th/0306034.
[10] M. Bleicher, SQM2003 proceedings.
[11] P. Granet *et al.*, Nucl. Phys. B **140**, 389 (1978).
[12] R.S. Longacre, nucl-th/0303068.
[13] P. Braun-Munzinger *et al.*, nucl-th/0304013.
[14] M. Anderson *et al.*, Nucl. Instrum. Meth. A 499, 659 (2003).
[15] C. Adams *et al.*, nucl-ex/0305015.
[16] C. Adler *et al.*, Phys. Rev. Lett. **87**, 112303 (2001).
[17] H. Albrecht *et al.*, Z. Phys. C **61**, 1 (1994).
[18] M. Derrick *et al.*, Phys. Lett. B **158**, 519 (1985).
[19] Y. J. Pei *et al.*, Z. Phys. C **72**, 39 (1996).
[20] V. Blobel *et al.*, Phys. Lett. B **48**, 73 (1974).
[21] R. Singer *et al.*, Phys. Lett. B **60**, 385 (1976).
[22] M. Aguilar-Benitez *et al.*, Z. Phys. C **50**, 405 (1991).
[23] D. Drijard *et al.*, Z. Phys. C **9**, 293 (1981).
[24] P.V. Chliapnikov *et al.*, Nucl. Phys. B **176**, 303 (1980).
[25] F.C. Winkelmann *et al.*, Phys. Lett. B **56**, 101 (1975).
[26] X.N. Wang and M. Gyulassy, Phys. Rev. D **44**, 3501 (1991); Compt. Phys. Commun. **83**, 307 (1994).
[27] C. Adler *et al.*, Phys. Rev. Lett. **89**, 272302 (2002).
[28] K. Hagiwara *et al.*, Phys. Rev. D **66**, 010001 (2002).
[29] F. Becattini, Nucl. Phys. A **702**, 336 (2002).
[30] P.D. Acton *et al.*, Z. Phys. C **56**, 521 (1992); G.D. Lafferty, Z. Phys. C **60**, 659 (1993).
[31] K. Ackerstaff *et al.*, Eur. Phys. J. C **5**, 411 (1998).
[32] D. Buskulic *et al.*, Z. Phys. C **69**, 379 (1996).